

Purdue University
Purdue e-Pubs

International Refrigeration and Air Conditioning
Conference

School of Mechanical Engineering

2012

Measurement of Mist to Annular Flow Development in the Discharge of a Compressor

Scott S. Wujek
scott.wujek@creativethermalsolutions.com

Predrag S. Hrnjak

Follow this and additional works at: <http://docs.lib.purdue.edu/iracc>

Wujek, Scott S. and Hrnjak, Predrag S., "Measurement of Mist to Annular Flow Development in the Discharge of a Compressor" (2012). *International Refrigeration and Air Conditioning Conference*. Paper 1325.
<http://docs.lib.purdue.edu/iracc/1325>

This document has been made available through Purdue e-Pubs, a service of the Purdue University Libraries. Please contact epubs@purdue.edu for additional information.

Complete proceedings may be acquired in print and on CD-ROM directly from the Ray W. Herrick Laboratories at <https://engineering.purdue.edu/Herrick/Events/orderlit.html>

Measurement of Mist to Annular Flow Development in the Discharge of a Compressor

Scott S. Wujek^{1*}, Predrag S. Hrnjak^{1,2}

¹Creative Thermal Solutions
Urbana, IL, USA
scott.wujek@creativethermalsolutions.com

²Air-Conditioning and Refrigeration Center
Department of Mechanical Science and Engineering
University of Illinois at Urbana-Champaign
Urbana, IL, USA
pega@illinois.edu

* Corresponding Author

ABSTRACT

Compressors produce a flow of oil droplets propelled by refrigerant flow while fully developed flow maps predict predominantly annular flow. This discrepancy is rooted in the lack of understanding of flow development. A newly developed video processing technique was used to quantify numerous flow parameters. The drop size, drop speed, drop concentration, film thickness, and film velocity were measured at a variety of refrigerant flow rates, oil circulation ratios, and temperatures. Measurements showing the changes in oil flow from the discharge of a compressor as a function of position are presented. An accompanying paper presents a model incorporating results from this experiment.

1. INTRODUCTION

Adiabatic annular-mist flows occur in round tubes at relatively high qualities and vapor flow rates. Complex interactions occur between the annular film, the vapor core, and the dispersed liquid droplets as shown in Figure 1. These interactions eventually lead to a fully-developed flow regime after which the annular film reaches a constant time averaged value and the rate of deposition equals the rate of entrainment. Flow visualization is commonly used in fluid dynamics, but it is rarely used to study the droplets in the core of annular flow because waves on the liquid film surface obscure the droplets.

Most research in multiphase flows has been either focused on fully-developed steady-state flows or else on fundamental studies on collision outcomes. While both of these areas have great utility for understanding multiphase flows, neither is relevant for many engineering applications. Flows generally take hundreds of tube diameters in order to become fully developed and positive displacement machines are incapable of providing a steady flow. Isolated, fundamental experiments, such as those where a single droplet strikes a quiescent film, are difficult to relate to the chaotic flow structure found in practice. The focus application of these experiments is air-conditioning systems, particularly automotive air-conditioning systems. While the understanding of flow fundamentals may be seen as important in its own right, one possible application for this study may be for use in improving the design of oil separators. The role of oil in the system is to lubricate the compressor, but it is detrimental to the function of almost every other component. Oil has been shown to impact heat transfer, pressure drop, and overall system performance, particularly in systems utilizing microchannel heat exchangers. This work should help design compact oil separators with a relatively small pressure drops and reasonably high efficiencies by giving designers insight as to how oil flows from the compressor. A good oil separator should keep the oil in the

compressor, where it is useful, and out of other system components. Currently, external oil separators are rarely used in certain applications due to associated pressure drop, size, weight, or initial cost.

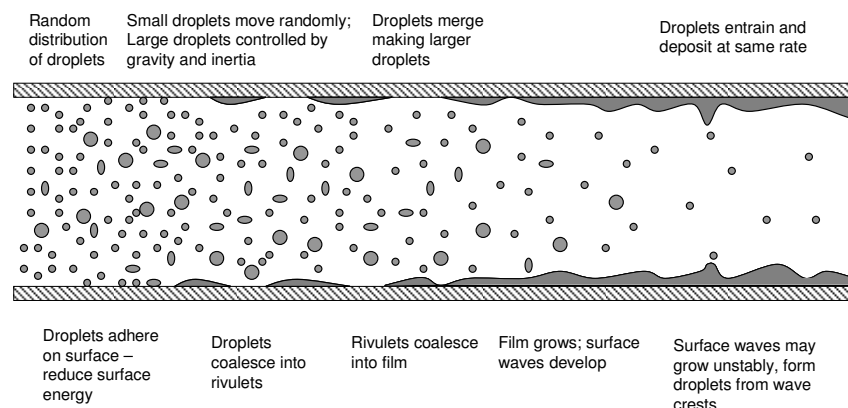


Figure 1: Flow interaction in adiabatic annular-mist flow

Due to its importance in refrigeration, electrical power generation, and chemical engineering, numerous researchers have studied droplet and annular film type flows. While many previous researchers have studied annular-mist two-phase flows there seem to be several noticeable gaps in the open literature:

- Most previous experiments in annular-mist flows have been conducted with a limited set of fluid combinations, with power generation as the desired application. Therefore, steam-water is the fluid pair of interest in those experiments. For ease and safety, flows involving this fluid pair are often studied in the laboratory environment using air-water or vapor R113-liquid R113. The properties of these fluids are vastly different to those of synthetic refrigerants and oils which are commonly found in air-conditioning and refrigeration applications.
- Due to difficulties in studying annular-flows many researchers have studied surrogates for the actual flow instead of actual annular-mist flows. This is especially true for visualization experiments. In order to gain some understanding of annular-mist flows, researchers have utilized tactics such as using solid particles instead of liquid droplets, removing the annular film, performing experiments on a flat plane instead of in a tube, or constructing complex inlet and exit sections. While each of these types of experiments have yielded valuable information about flow dynamics, in many cases the results have not been properly compared to actual annular-mist flows.
- Most previous work has been focused on fully-developed flow regimes. In applications such as air-conditioning however, it is rare that the necessary tubing length for achieving fully-developed flow is found. Therefore, it is important to study how the liquid flow develops from droplets produced by the compressor to oil adhering to the wall surface.

2. EXPERIMENTAL FACILITY

A compressor is used to provide the flow of liquid and vapor. The focus of this experiment facility is on the compressor discharge line, which is described in detail later. A thermodynamic cycle consisting of the typical air-conditioning components was constructed. A schematic of the experimental facility can be found in Figure 2. The relative location of the various refrigerant side measurements are shown, along with locations of the most critical air side measurements. Temperatures and pressures of the fluid streams passing through each component are measured.

The open-shaft automotive compressor used in this experiment was fairly typical for automotive systems. The compressor was a wash-plate type design containing 10 compression chambers. The rationale behind using this type of compressor was that the open shaft design and lack of an oil sump simplified the process of altering the compressor speed and oil circulation ratio, respectively.

The facility is designed in such a way as to minimize flow disturbance after the compressor discharge. The compressor discharge tube has an internal diameter of 6.35 mm and is made of a transparent perfluoroalkoxy (PFA) tube. This material is chemically similar to polytetrafluoroethylene (PTFE) but is transparent. The length of the tube exceeds the length-to-diameter ratio of 480 suggested by various articles to ensure that the flow is fully

developed. Surface properties of the tube, such as wettability and roughness, will not match those of the metal tubing typically used, the overall geometry of air-conditioning or refrigeration components are replicated by the plastic tubing. Wettability should not limit the application of the experimental results so long as the entire surface is coated by the liquid film. Likewise roughness effects should be minor so long as the film is laminar and the roughness is small compared to the film thickness.

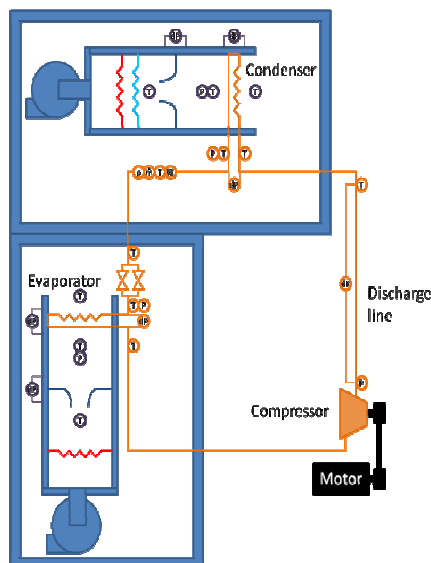


Figure 2: Schematic of the experimental facility

Due to the high speed of droplets and waves in the annular film, a high speed Vision Research SR-CMOS camera was utilized to record images of the flow. For these experiments a framing rate of roughly 11,000 frames per second is used with a resolution of 384 by 128 pixels. The high framing rate and short exposure time allows for individual droplets and waves to be tracked over a series of frames while still being able to determine the drop size with relatively high accuracy. Due to short exposure times and high magnification, very intense light is required. The tube is backlit with a 150W halogen light which is transmitted through fiber optics. The discharge end of the fiber optics is positioned to emit an intense light positioned roughly 30 mm from the tube on the side opposite the camera. Since the light emanates from a single point, a translucent white diffuser is utilized to reduce glare. Due to the large aspect ratio of the tube and the small area being filmed at a given time, it is necessary to move the camera, lens, and light source to film the entire length of tube. A jig is used to precisely align the camera, lens, tube, and light source. The jig is required as slight changes in relative positioning of the light, tube, and camera can cause the flow to appear dramatically differently.

Film thickness is measured using a critical angle approach suggested by Hurlburt and Newell (1996) and subsequently improved by Shedd and Newell (1998). An optical model was constructed by Wujek (2011) which allowed film thickness to be calculated from elliptical rather than flat cross sections. The advantages of measuring on elliptical cross sections include faster sampling and greater precision. The high speed camera is used to detect the light circle formed by light from a laser reflecting off of the liquid-vapor interface. For film thickness measurements, the high speed camera was run at a frame rate of approximately 3000 frames per second and a resolution of 320 by 512 pixels with an exposure time of up to 100 μ s. The critical angle method for determining film thickness has several advantages which are discussed in further detail in the chapter on film thickness measurement.

Only in the liquid line do the refrigerant and oil flow together as a single phase, which makes it the ideal location in the system for measuring the ratio of oil to total flow rate, which is called the oil circulation ratio (OCR). Additionally, the liquid line contains means for online measurement of density and index of refraction for purpose of determining the relative flow rates of the two components in the mixture. To reinforce the online measurements of oil circulation ratio, a valve was installed for the purpose of pulling liquid samples as recommended by ASHRAE Standard 41.4.

3. TEST CONDITIONS

The overall range of test conditions conducted as part of this research was for mass flow rates of 6.3 to 22 g/s, oil circulation ratios from 1.1 to 18.5%, discharge temperatures 44 to 103°C, discharge pressures from 1025 to 1375 kPa, liquid viscosities from 4 to 19 cP, and vapor densities from 26 to 54 kg/m³. The change in fluid properties is a result of the liquid phase properties of R134a-PAG oil mixtures. Liquid phase properties were determined using correlations developed by Seeton (2009).

While all of these experimental test conditions were used to understand the impact of different operating conditions on fluid flow, this paper outlines the results obtained using the new optical method for measuring various parameters within annular-mist flow and the method for measuring film thickness in round tubes for one specific test condition. The limitation on the amount of data presented is necessary due to page restraints, the full complement of data may be found in Wujek (2011).

The results for this condition were relatively typical, and similar analysis was done for every other flow condition. The conditions measured in this discharge line were a temperature of 103° and a pressure of 1381 kPa. The mass flow rate was measured to be 21.2 g/s. At these conditions the bulk velocity of the vapor refrigerant is 12.5 m/s. The compressor frequency was determined based on readings from the frequency drive, motor information, and pulley ratio. The compressor frequency was calculated to be 30.3 Hz, meaning that one of the compressor's chambers completes a cycle every 3.3 ms. From measured values, the oil circulation ratio was found to be 4.5%, meaning the oil flow rate was approximately 1.1 g/s.

4. EXPERIMENTAL RESULTS

While many details of the liquid component of the flow can be measured with the newly developed techniques, only those which are most important for understanding the flow development are mentioned here. These important parameters are the drop size, the drop velocity components in the axial direction and in an orthogonal direction, the drop concentration, the film speed, and the film thickness are discussed in this paper.

4.1 Drop size distribution

The size of drops along the length of the tube was measured utilizing an edge transition technique based on the work of Hay *et al* (1998). At each location along the tube, the video is analyzed with this method and a drop size distribution is created. A drop size distribution is similar to a histogram in that it gives an understanding of the relative prominence of drops of different diameters. Figure 3 can be thought of as a series of drop size distributions stacked next to each other so that the cross section of the surface at a given downstream position gives the mass distribution of droplet sizes. While the raw data produces relatively consistent results, the data shown in Figure 3 has been smoothed to iron out slight inconsistencies from one location to the next. The fully developed volume mean drop size was determined to be approximately 45 μm.

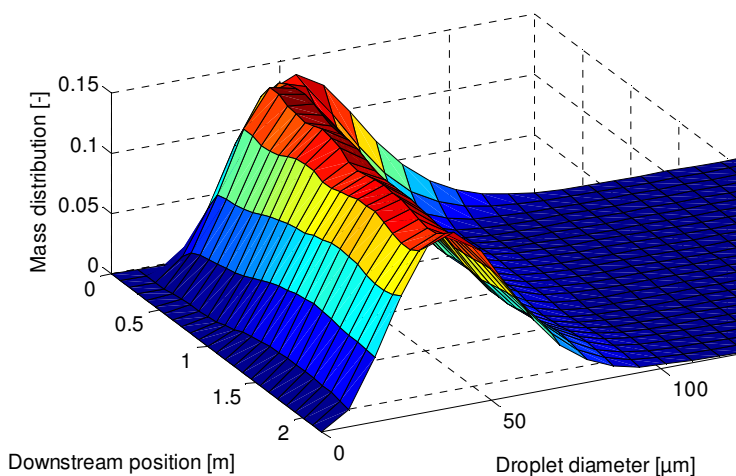


Figure 3: Development of drop mass distribution

There are a few noticeable trends in the drop size distribution. First, the peak in the initial mass distribution of drop sizes is slightly larger than the fully-developed peak. Second, the peak diameter undergoes a rapid transition to smaller drops in the first 0.25 m of the tube, and then undergoes subtle transition to slightly smaller drop sizes. Third, the drop size distribution resembles the upper-limit log-normal distribution which is consistent with the findings of other researchers. With a mass distribution such as this, very little mass is contained in either the smallest or the largest droplets found in the flow.

Changes in drop size distribution are the result of a few processes. The drop size distribution is the cumulative result of drops of different sizes undergoing one of the following four interactions at different frequencies. The first such interaction is that some drops which were in the flow deposit on the wall surface. Second, large drops may split into smaller drops as a result of Taylor instabilities (Karam and Bellinger, 1968). Third, high viscosity droplets tend to merge on impact with one another (Gotaas *et al* 2007). Fourth, new drops are entrained from the liquid film. This entrainment is typically the result of instabilities at the surface of disturbance waves (Tattersson , 1975).

4.2 Drop velocity development

Two components of drop velocity are fundamentally important to the flow development. First, the axial component is important because this is used to determine the mass flux of the drop phase. Second, the radial component is important because this motion is responsible for drop collisions with the liquid film on the tube wall. As the video used in the analysis is filmed from alongside the tube, the axial velocity is measured via the vertical velocity. The speed of a drop of fixed mass is determined by two parameters, its initial speed and the forces acting upon it. While weight is an important force in the vertical direction, the only important force in the horizontal direction is drag.

Experimental results for drop axial velocity development are shown in Figure 4. This result is created by combining the droplet velocity histograms for a given condition created from video recorded at a series of downstream locations. From Figure 4, a few trends are noteworthy. One, there is a dominant peak in drop speed distribution which occurs at roughly 80% of the vapor velocity. Two, the dominant peak in the distribution becomes shorter and wider. Three, a second peak develops at a low velocity. Four, the initial drop velocity appears to be larger than the fully developed drop velocity.

Many of these trends make a great deal of physical sense for the experimental system studied. The narrow distribution of drop speeds at the beginning is most likely due to the fact that a large percentage of the drops are generated in the same manner within the exit regions of the compressor. Because the flow is generated by cyclical means, the bulk vapor flow rate is not steady. The drop speed distribution becomes wider because the drops experience cyclical shear forces from the vapor. The secondary peak in the size distribution is due to the generation of drops from the relatively slow moving film. The frequency of drop generation is proportional to film flow rate; the film flow rate is negligible at the beginning of the tube. The initial drop velocity may be higher due to the fact that initially, the drops are created at the compressor discharge valve. At the discharge valve, the velocity is higher because the cross-section through which the flow passes is much smaller.

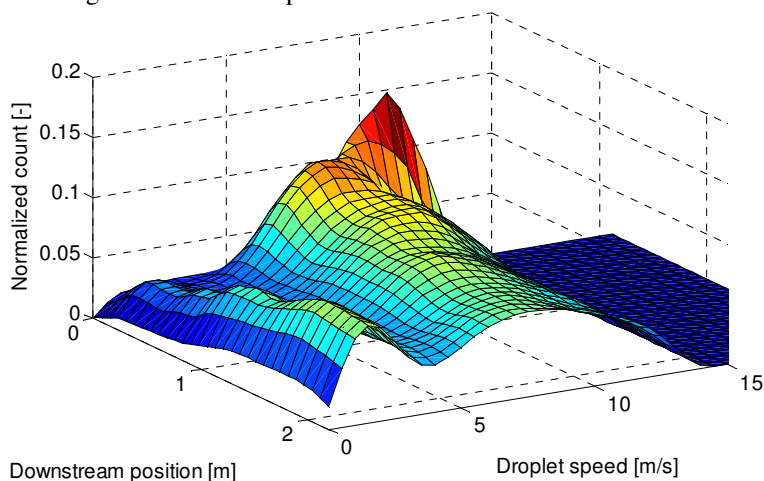


Figure 4: Development of the drop axial velocity distribution

Figure 5, shows the distribution of the vertical component of droplet velocity. The vertical velocity distribution is nearly Gaussian and only shows a slight broadening with downstream position. The average velocity, which is near the peak, begins in the slightly upward direction and transitions to being slightly downward. It can be seen that the initial change in drop upward velocity is similar to the initial drop size. The main reason for this steep change in drop velocity is due to large, upward moving, drops depositing on the upper surface of the tube. After this point, the slight downward trajectory is caused by the weight of the particles. Unlike with the large initial drops, the velocity for the small drops is easily affected by turbulence, which has the tendency to randomize the location of the drops in the vertical direction. However, the bulk motion of the drops is slightly downward.

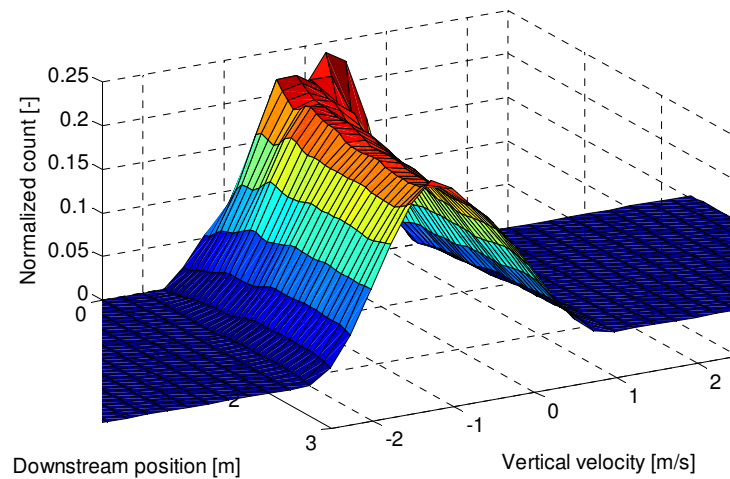


Figure 5: Development of drop vertical velocity distribution

4.3 Drop concentration development

The way in which the quantity of droplets in the flow is generally presented in multi-phase flow literature is by droplet concentration. There are two major reasons why the amount of droplets is typically reported in terms of concentration instead of as a number density. First, no matter what method is used, it is difficult to find the smallest droplets in the flow. Second, these small droplets are of little interest to engineers because their small mass means the impact of their extensive properties are of little concern when calculating issues relating to energy or mass transport. The methodology for how drop concentration is determined by video analysis can be found in Wujek (2011). The combined effects of drop entrainment and deposition can be seen in Figure 6. It can be seen that the concentration of droplets in the vapor seems to decrease rapidly in the first 0.5 m, followed by a more gradual decrease for the remainder of the tube.

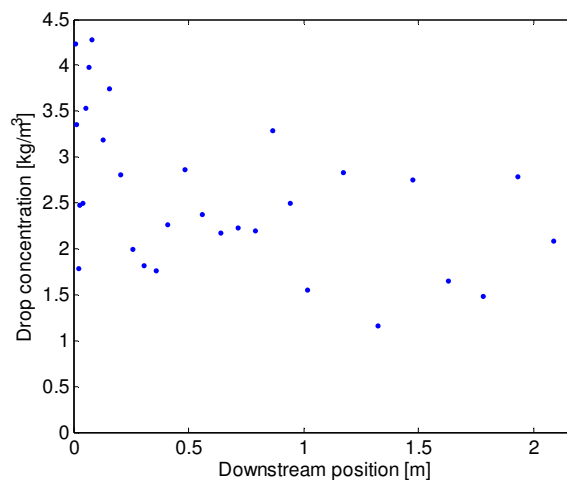


Figure 6: Development of drop concentration

4.4 Wave speed

The waves in the liquid film progress down the tube in the direction of flow. The wave motion is an important mode by which the liquid flows in the tube. The average wave speed at several downstream locations was determined as shown in Figure 7. It can be seen that the film continues to be accelerated as it flows down the tube. There is a sharp increase in wave speed near the beginning of the tube, then a nearly linear function with respect to position after about 0.5 m. It should be noted that the wave speed is the speed at which the surface of the liquid film travels. The bulk speed of the film is an average between the boundary conditions given by the wave motion and the wall.

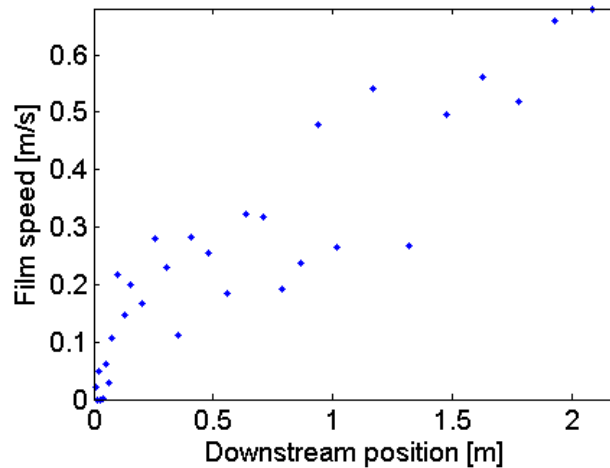


Figure 7: Development of film speed

4.5 Film thickness and wavelength

The liquid film is often considered to be comprised of two layers: wave and base. The wave layer is comprised of the ripple or disturbance waves which are carried down the tube at a relatively high velocity. The entire mass of the wave is generally considered to move at a uniform speed. The base layer is between the wave layer and the tube wall. This layer has a velocity profile dependant on radial position while the fluid next to the wall has a negligible velocity while the other surface moves at the wave velocity.

The liquid film thickens as a function of downstream position. The base film thickness and the wave height measured at several downstream positions can be seen in Figure 8. It can be seen that the wave height remains relatively constant while the base layer thickens as the flow develops. The average film thickness can be calculated by adding the base height plus the wave height. Initially, the film thickness appears to be approximately $45\ \mu\text{m}$. The film grows until reaching a fully developed film thickness of $135\ \mu\text{m}$. Unfortunately, there appears to be a random error of approximately $25\ \mu\text{m}$, which is approximately $1/6$ of the fully developed film thickness.

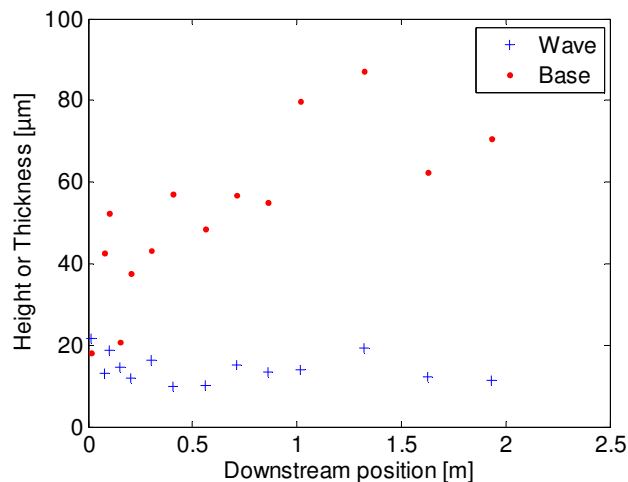
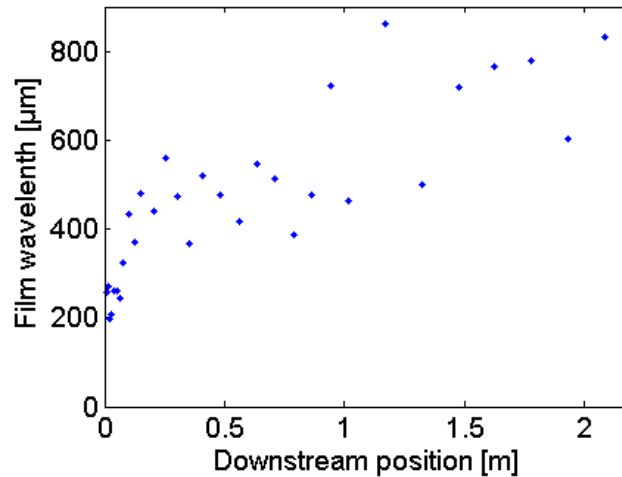


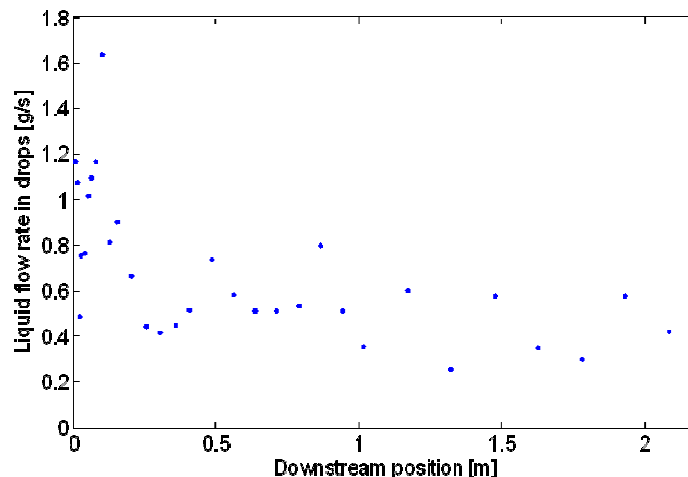
Figure 8: Development of film thickness

Wavelength tends to grow as the flow progresses down the tube, as can be seen in Figure 9. Ambrosini (1991) showed that wavelength is proportional to film thickness for a given film Reynolds number. A similar trend is found by comparing the experimental film wavelength with the values recorded for the base film height. It should be remembered that film thickness is calculated using a different video, therefore any temporal changes in the flow would not be accounted for.

**Figure 9:** Development of film wavelength

4.6 Liquid mass distribution

By combining the experimental flow data and fluid properties, it is possible to determine the mass flow rate of liquid drops in the flow. By combining, drop concentration, drop velocity, and tube geometry, it is possible to determine the mass flow rate of liquids in the form of drops. Figure 10 shows the drop mass flow rate as calculated from these terms. It can be seen that the mass flow rate of liquid which is in the form of drops decreases rapidly near the beginning of the tube then remains relatively steady. The initial flow rate in the drops is approximately 1.2 g/s while the fully developed mass flow rate is about 0.5 g/s. The difference between the initial and fully developed mass flow rates must be compensated by a simultaneous increase in the flow rate in the liquid film.

**Figure 10:** Development of drop flow rate

The liquid film flow rate can be estimated by combining information for the wave speed and film thickness measurements. To accomplish this, the velocity profile inside the film must be estimated. If a laminar profile in the film is assumed, then the profile can be approximated by a linear variation in velocity with respect to radial position.

Typically, the film is divided into a base-film and a wave component. In these models, the wave moves at the wave velocity, but the base film moves at a separate, and much lower, velocity. The base film velocity is typically modeled as moving at a velocity equal to the thickness of the base film would then be given by the minimum film thickness. It is necessary to know the dimensions of the wave, so that the volume of fluid transported in each wave can be approximated. The volume of wave can be found by integrating the difference between the film thickness and the base film thickness. One difficulty with models which separate the wave from the base film is determining the base film velocity. Generally, the total liquid flow rate is known and the velocity of the base film is solved using a continuity equation. This approach was taken by Han, Zho, and Gabriel (2006). They found that the base film moves at approximately 1/14 of the velocity of the waves. Experimental tracking of dye in annular films by both the base film and by wave motion are given by Sutharshan, Kawaji, and Ousaka (1995). It appears from their limited experimental runs that the base film traveled at approximately 2/5 of the disturbance wave speed. If these ratios hold, the volume film flow (\dot{V}) rate would be approximated by Equation 1, where C represents the ratio of base film to wave velocity, D is the tube diameter, u_w is the wave velocity, δ is the height of the wave peak, and δ_b is the base film thickness. The linear profile would have a value of C equal to 1/2.

$$\dot{V} = 2\pi D \bar{u}_w \left(\frac{\max(\delta) - \delta_b}{2} + C \delta_b \right) \quad (1)$$

Mass flow rate in the film is calculated based on experimental measurements of film thickness and film speed. Using Equation 1, it was found that the value of $C=0.4$ showed relatively good agreement with experimental results. The development of liquid flow rate in the film as calculated using these equations can be seen in Figure 11. Near the beginning of the tube, the waves were nearly stationary so it is believed that there is initially no mass flow in the film. As the vapor shear acts on the liquid, waves begin to be pushed down the tube. Simultaneous with this wave movement, the film thickens due to deposition of droplets. However, because mass is conserved, the model for liquid film flow rate can be arrived at by subtracting the drop flow rate at any point from the total liquid flow rate.

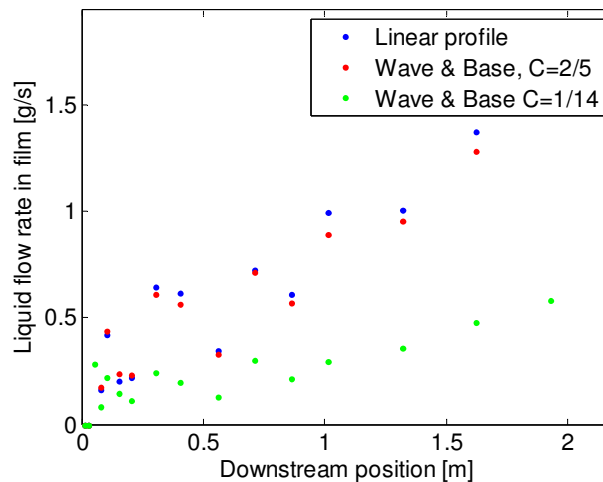


Figure 11: Development of film flow rate based on 3 velocity profiles

The distribution of liquid mass flow between droplets and film develops as a result of the net effects of entrainment and deposition. Entrainment is when liquid is sheared from the film and is transformed into droplets, while deposition occurs when drops strike the film and become absorbed. As the quantity of liquid remains relatively constant, the total of the droplet and film flow rates should also remain constant. As the liquid enters the tube, it is comprised primarily of a mist of droplets. While the wall is wetted, there is little measureable film flow at the tube entrance. The combined effects of drop entrainment and deposition are shown in Figures 10 and 11. The total mass flow rate at each location was constant to within the accuracy of measurement and was near the total liquid flow rate calculated using mass flow and oil circulation ratio measurements.

5. CONCLUSIONS

Using recently developed visualization techniques, it is possible to determine several important flow parameters in two phase flow from high speed videos. By traversing the length of the tube with the camera, flow development can be studied by comparing videos recorded at several locations. Among the key observations it was found that large droplets preferentially deposit near the tube entrance. After this initial region, the drop mass distribution skewed to slightly smaller drops as the flow progressed. While compressors produce an approximately Gaussian distribution of drop velocities, the axial velocity develops into a bimodal distribution of velocities. This distribution is evidence that droplets are being entrained from the oil film which coats the surface of the tube. On average, the drops slowly fall due to the effects of gravity. The flow of liquid transitions from being predominantly in small droplets to flowing as a film on the tube wall. An effect of this is that the film becomes thicker while simultaneously moving faster. Models which fit the experimental results as well as a large data set of results from other experimentalists can be found in the accompanying paper.

REFERENCES

- Ambrosini, W., Andreussi, P, and Azzopardi, B., 1991, A physically based correlation for drop size in annular flow, *International Journal of Multiphase Flow*, 17, 497-507.
- Gotaas, C., Havelka, P., Jakobsen, H., Svendsen, H., Hase, M., Roth, N., and Weigand, B., 2007, Effect of viscosity on droplet-droplet collision outcome: experimental study and numerical comparison, *Physics of Fluids*, 19, 102106-1-102106-17.
- Han, H., Zhu, Z., & Gabriel, K. 2006, A study on the effect of gas flow rate on the wave characteristics in two-phase gas-liquid annular flow: *Nuclear Engineering and Design*, 236, 2580-2588.
- Hay, H., Liu, Z., & Hanratty, T., 1998, A backlighting imaging technique for particle size measurements in two-phase flow, *Experiments in Fluids*, 25, 226-232.
- Hurlburt, E. and Newell, T., 1996, Optical measurement of liquid film thickness and wave velocity in liquid film flows, *Experiments in Fluids*, 21, 357-362.
- Karam, H. and Bellinger, J., 1968, Deformation and breakup of liquid droplets in a simple shear field, *Industrial and Engineering Chemistry Fundamentals*, 7, 576-581.
- Seeton, C., 2009, *CO₂-lubricant two-phase flow patterns in small horizontal wetted wall channels; the effects of refrigerant/lubricant thermophysical properties*, University of Illinois, Urbana.
- Shedd, T. and Newell, T., 1998, Automated optical liquid film thickness measurement method, *Review of Scientific Instruments*, 69, 4205-4213.
- Sutharshan, B., Kawaji, M., and Ousaka, A., 1995, Measurement of circumferential and axial liquid film velocities in horizontal annular flow, *International Journal of Multiphase Flow*, 21, 193-206.
- Tatterson, D., 1975, *Rates of Atomization and Drop Size in Annular Two-Phase Flow*, University of Illinois, Urbana.
- Wujek, S., 2011, *Mist to annular flow development quantified by novel video analysis methods*, University of Illinois, Urbana.

ACKNOWLEDGEMENT

The authors of this paper acknowledge the support of the member companies of the Air-Conditioning and Refrigeration Center at the University of Illinois at Urbana-Champaign.